

INFLUENCE OF A FOREST CANOPY ON THE NEUTRAL ATMOSPHERIC BOUNDARY LAYER - A LES STUDY

B. Nebenführ^{1,2} and L. Davidson^{1,2}

¹ *Div. of Fluid Dynamics, Dept. of Applied Mechanics,
Chalmers University of Technology, Gothenburg, Sweden*

² *SWPTC, Swedish Wind Power Technology Center*

bastian.nebenfuhr@chalmers.se

Abstract

Large-eddy simulation was used to investigate the influence of a forest on the neutral atmospheric boundary layer. This can yield important information for the design and placement of wind turbines in forest regions. Two simulations were conducted: one with and one without the forest. The simulation with forest showed good agreement with field measurements. It was found that the forest significantly increases both the wind shear and the turbulence intensity at the hub-height of an imaginary wind turbine. Both quantities clearly exceed the recent wind turbine design criteria.

1 Introduction

Placement of wind turbines in forest regions is becoming increasingly interesting. As the forest can help to mitigate visual and audible effects of wind turbines, that often lead to rejection of wind parks by local residents, it is easier to get a permit for developing a wind park inside a forest than for possible sites near residential areas. The advent of tall wind turbine towers of above 100m makes it possible to operate wind turbines efficiently even in the fairly low wind speeds encountered above forests. Additionally, maintenance and grid connection are simplified compared with off-shore wind parks. However, it has been found that the wind conditions above forests are characterized by strong wind shear and increased turbulence levels. As a consequence of the strong turbulence, wind turbines in forest regions are exposed to strong fluctuating aerodynamic loads, while the increased wind shear leads to strong cyclic loading. Forest regions therefore provide a hostile environment even for the strongest available wind turbines, leading to a shortened fatigue life and increased maintenance requirements.

Large-Eddy Simulation (LES) can be used to simulate the atmospheric boundary layer (ABL) under the influence of a canopy. This numerical analysis provides valuable insight into the characteristics of forest turbulence and the fluctuating aerodynamic loads encountered by the wind turbine. Based on this knowledge, design criteria for wind turbines in forest regions can be adapted and the placement of future wind tur-

bines can be optimized.

Already since the 1970's (Deardorff, 1972; Sommeria, 1976), LES has successfully been employed for the simulation of ABL flows. In the initial development, the influence of different terrains was taken into account in terms of wall functions based on the Monin-Obukhov similarity theory. These wall functions prescribe the wall shear stress corresponding to a certain surface roughness length. A variety of terrains can be simulated simply by adjusting the roughness length. Above short vegetation and low roughness surfaces, it might be appropriate to represent the terrain using roughness wall functions. However, the permeability of the roughness elements in case of more extreme terrain, such as forests, should be taken into consideration and the possible effects of the interaction of flow inside and above the roughness elements should be included in the simulations. Shaw and Schumann (1992) conducted the first LES study in which the forest was explicitly accounted for. In that simulation, the forest was represented in terms of a drag force exerted by the trees on the flow. Since then many research groups have used this technique to investigate different aspects of canopy flows. Two focal points that gained great attention are the simulation and recognition of coherent structures (Kanda and Hino, 1994; Watanabe, 2004; Dupont and Brunet, 2009) and the simulation of clearing-forest-clearing type of patterns for the study of canopy-edge influences (Dupont and Brunet, 2008a; Dupont et al., 2011).

In this paper, first the methodology of forest LES is presented. In order to study the influence of the forest, two LES of the neutral ABL are conducted: One with and one without the forest present. The simulation with forest is then validated against field measurements. Finally, it is pointed out how the ABL is changed by the presence of a forest and what implications these changes may have from a wind turbine point-of-view.

2 Simulation setup

In our LES, the incompressible, filtered Navier-Stokes equations are solved. The effects of the Earth's

rotation, which gives rise to the Coriolis effect, and the forest canopy are taken into account through source and sink terms in Eq. (1).

$$\frac{\partial \bar{u}_i}{\partial t} + \frac{\partial(\bar{u}_i \bar{u}_j)}{\partial x_j} = -\frac{1}{\rho} \frac{\partial \bar{p}}{\partial x_i} + \frac{\partial}{\partial x_j} \left[(\nu + \nu_t) \frac{\partial \bar{u}_i}{\partial x_j} \right] + F_i \quad (1)$$

where ρ is the fluid density, ν and ν_t are the molecular and eddy viscosity, respectively, \bar{u}_i ($u_1 = u$, $u_2 = v$, $u_3 = w$) are the instantaneous velocity components and \bar{p} is the pressure. Filtered quantities are denoted by overbars.

The source/sink terms are included in F_i and read:

$$F_i = F_{forest} + F_{coriolis} = -C_D a_f V \bar{u}_i - 2\Omega \sin(\phi) (\bar{u}_k - u_{k,g}) \varepsilon_{i2k} \quad (2)$$

where the first term is the forest sink term and the second term is the source/sink term due to the Coriolis effect. The forest drag term in Eq. (2) is written in a way similar to Shaw and Schumann (1992). It is composed of the drag coefficient, $C_D = 0.15$, (Shaw et al., 1988), the forest dependent leaf-area density (LAD) profile, a_f , the local velocity magnitude, V , and the instantaneous velocity component, \bar{u}_i . The Coriolis term is comprised of the Earth's rotational velocity, Ω , the latitude ϕ (here taken as $\phi = 57^\circ$, corresponding to southern Sweden), the velocity component, \bar{u}_k , and the geostrophic wind component, $u_{k,g}$. A geostrophic wind of $(u_g, w_g) = (10, 0) m/s$ is chosen. The geostrophic wind will cause a pressure gradient in the lateral direction, which, when balanced by the Coriolis force, drives the flow. Additionally, it leads to height dependent turning of the wind.

Sub-grid scale (SGS) turbulence is parameterized using a k -equation model similar to the one proposed by Deardorff (1980). The transport equation of the turbulent kinetic energy reads:

$$\frac{\partial k}{\partial t} + \frac{\partial(\bar{u}_j k)}{\partial x_j} = \frac{\partial}{\partial x_j} \left[\left(\nu + \frac{\nu_t}{\sigma_k} \right) \frac{\partial k}{\partial x_j} \right] + P_k - \varepsilon - \varepsilon_f \quad (3)$$

where $\sigma_k = 1$ and

$$P_k = \nu_t \left(\frac{\partial \bar{u}_i}{\partial x_j} + \frac{\partial \bar{u}_j}{\partial x_i} \right) \frac{\partial \bar{u}_i}{\partial x_j} \quad (4)$$

$$\varepsilon = \frac{C_\varepsilon k^{3/2}}{l}$$

$$\varepsilon_f = \frac{8}{3} C_D a_f V k$$

are the production of turbulent kinetic energy, its dissipation rate and a sink term to account for the forest, respectively. The coefficient C_ε is set to 0.93 as in

Shaw and Patton (2003) and the filter length is taken as the cubic root of the cell volume, $l = (\Delta_x \Delta_y \Delta_z)^{1/3}$. Finally, the eddy viscosity is calculated according to Eq. (5).

$$\nu_t = 0.1 l \sqrt{k} \quad (5)$$

In the simulations, a rectangular domain with the dimensions $(x_{max}, y_{max}, z_{max}) = (4H, H, 2H)$ is used, where $H = 400m$ is the vertical domain height. This domain is divided into $(192, 96, 96)$ cells. The forest canopy covers the lowest 10 cells of the domain and has a constant height of $h = 20m$. The grid spacing in the horizontal directions (x and z) is constant. Inside the forest, the vertical cell size is kept constant at $\Delta_y = 2m$. Above the forest, the cells are geometrically stretched by 1.7%. The forest is modeled as being horizontally homogeneous, i. e. the LAD profile is only dependent on the y -direction. At the ground, the wall shear stress, τ_w , is specified based on a surface roughness length. The commonly used Monin-Obukhov similarity theory is applied, which leads to Eq. (6).

$$\tau_w = - \left(\frac{u_{par} \kappa}{\ln(y/y_0)} \right)^2 \quad (6)$$

where $u_{par} = (\bar{u}^2 + \bar{w}^2)^{1/2}$ is the instantaneous horizontal velocity magnitude evaluated at the first grid point, $y = \Delta_y/2$ and $\kappa = 0.41$ is the von Karman constant. The surface roughness length is specified as $y_0/h = 0.001$ according to Shaw and Schumann (1992). With the given canopy height, this can be understood as a grass covered surface below the forest (Wieringa, 1992). In the streamwise and lateral direction, periodic boundary conditions are employed and the upper end of the domain is treated as a rigid, frictionless lid. The time-step is chosen to be $\Delta t = 0.4s$, which ensures $CFL < 0.5$ in the entire domain.

Extensive measurements have been made in a forest near Rynningsnäs in southern Sweden. Data from these measurements are used here for validation. The measurement campaign took place during the course of two years using a meteorological mast of height 140m, equipped with a measurement boom each 20m. The lowest boom was installed at a height of 40m. Detailed information and analysis of the measurements can be found in the final report of the Vindorsk project (Bergström et al., 2013). The forest in Rynningsnäs is comprised mainly of Scots pine trees (*Pinus sylvestris*). With the help of the empirical model of Lalic and Mihailovic (2004), the LAD profile in Fig. 1 was generated. It exhibits a dense crown and a less obstructed trunk region. The leaf-area index (LAI) of the profile is $LAI \approx 4.3$. Breuer and co-workers show in their review paper (Breuer et al., 2003) that the leaf-area index for a Scots pine varies between $LAI \approx 1.1 - 7.2$ with the mean value at around 3.8.

The simulation without forest has been carried out under the exact same circumstances as described

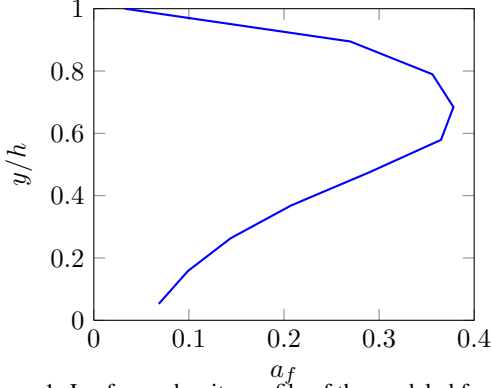


Figure 1: Leaf-area density profile of the modeled forest.

above. The forest is then disregarded by means of deactivating the sink term. Essentially, this means that the simulation without the forest can be understood as being representative of the atmospheric boundary layer over grass-covered terrain.

Both simulations are carried out for neutral atmospheric stability. That means that no heat exchange between the forest and the air is considered and hence buoyancy effects can be neglected.

A coordinate transformation to a local coordinate system is applied for most of the quantities presented in this study. This is in order to account for the wind turning induced by the Coriolis effect. In line with common meteorological practice, the x -axis of the local coordinate system is aligned with the mean wind direction at every height and the y -axis is vertically upwards.

3 Comparison with measurements

In order to validate the LES including the forest, first and second moment statistical quantities are compared to field measurements. Figure 2 displays the profile of horizontal wind speed, $M = \sqrt{\bar{u}^2 + \bar{w}^2}$, normalized with the friction velocity, $u_* = (\bar{u}'v' + \bar{v}'w')^{1/4}$ evaluated at $y/h = 2$. The normalization of the quantities in this section is carried out in accordance to the measurements. The green shaded area in this and the following figures indicates the region of the canopy. It can be seen that the LES is in good agreement with the measurements. The wind speed profile exhibits the shape typical for canopy flows, with a strong retardation within the canopy and an inflection point at the top of the canopy. The presence of the inflection point in the profile has motivated the interpretation of canopy flows in terms of a mixing layer rather than a surface layer (Raupach et al., 1996, Finnigan, 2000).

Also the vertical shear stress, as given in Fig. 3, is in good agreement with the measured values. It can be seen that the shear stress is rapidly reduced to very small values inside the canopy. The maximum shear stress appears right at the top of the canopy. With increasing height, the shear stress then decays until the

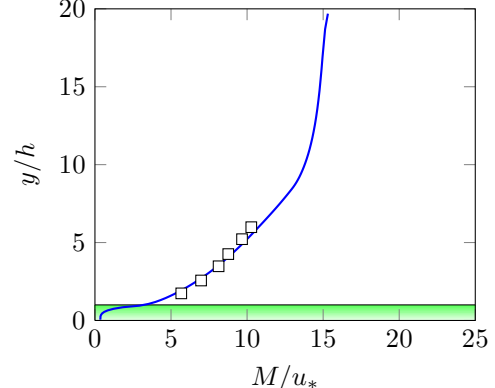


Figure 2: Horizontal wind speed profile. \square : Measurements (Bergström et al., 2013), —: LES

zero value, corresponding to the slip condition at the upper boundary.

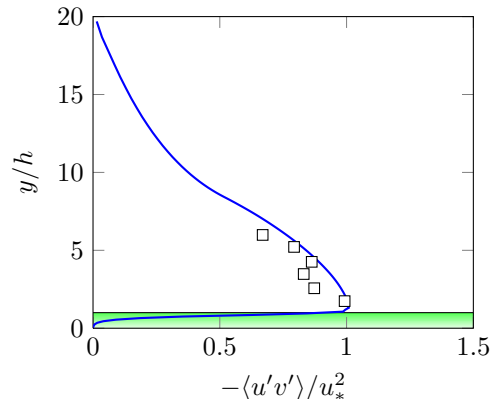


Figure 3: Shear stress profile. \square : Measurements (Bergström et al., 2013), —: LES

Profiles of the three normal stresses are presented in Fig. 4 along with field measurements. The stresses in the streamwise and lateral directions are the largest. Due to the presence of the ground, the vertical stress is damped and shows the smallest values. It can be noted that the vertical stress agrees well with the field measurements. The slight over- respектив under-prediction of the stresses in the streamwise and lateral directions is caused by the fact that LES predicts lower wind turning angles than measured in the field. Figure 5 shows the underprediction of the measured wind turning angles by the simulations, particularly for the region further away from the canopy. However, it has been argued that the measurements may yield too large wind turning angles due to internal twisting of the measurement tower (Bergström et al., 2013). Note that the angles in Fig. 5 are given relative to the wind direction at $y/h = 2$. The same figure also suggests that there is a strong wind turning within the canopy. These findings are confirmed by Dupont and Brunet (2008a), who show angles of up to 60° inside the forest. They also point out that the wind turning is highly dependent on the LAD profile. Since the wind speed is very small inside the canopy, the effect cannot directly be related to the Coriolis force. Dupont and Brunet (2008a) argue that the shear stress van-

ishes as a result of the canopy and that the flow aligns with the large-scale pressure gradient induced by the geostrophic wind. Hence, the strong wind turning inside the forest is only indirectly caused by the Coriolis effect. In terms of a wind turbine, it is noteworthy that the wind direction is changed by roughly 5° over a typical rotor diameter in the neutral atmospheric conditions considered here.

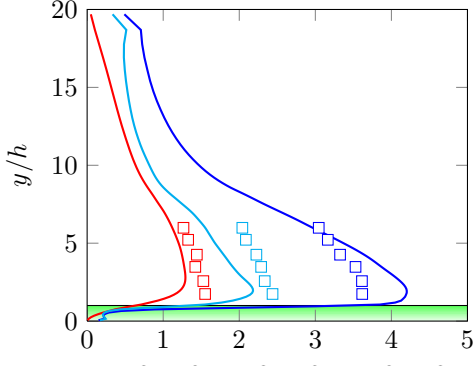


Figure 4: Normal stress profiles. Measurements (Bergström et al., 2013): □: streamwise, ▢: vertical, □: lateral; LES: —: streamwise, —: vertical, —: lateral

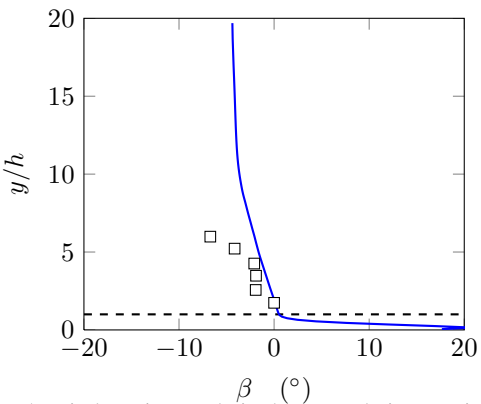


Figure 5: Wind turning angle in degrees relative to wind direction at $y/h = 2$. □: Measurements (Bergström et al., 2013), —: LES

4 Influence of the forest

The initial hypotheses were that the presence of the forest would lead to both stronger wind shear and increased turbulence levels above the forest. To prove the first hypothesis, the horizontal wind speed profiles of two identical LES with and without the forest are presented in Fig. 6. For clarification, a fit of the wind profile following the power-law function given by Eq. (7) is also included in the graph.

$$u(y) = u_{ref} \left(\frac{y}{y_{ref}} \right)^\alpha \quad (7)$$

In the above equation, y_{ref} is a reference height (here taken as the hub-height of an imaginary wind turbine,

$y/h = 4.5$) and u_{ref} is the wind speed at that reference height. The exponent α is the wind shear exponent for which the IEC suggests $\alpha = 0.2$ as a design criterion for modern wind turbines (IEC, 2005). For the with- and without-canopy cases, the exponents used for fitting the profiles in Fig. 6 are set to $\alpha = 0.52$ and $\alpha = 0.19$, respectively. Thus, the with-canopy case clearly exceeds the design criterion. Using identical boundary conditions in the with- and without canopy cases, the wind speed profile of the forest case does not reach as high values as the case without forest. This is due to the additional sink term in the momentum equations in the forest case.

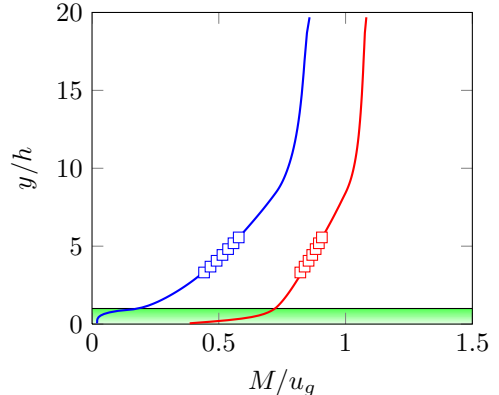


Figure 6: Horizontal wind speed profile normalized with the geostrophic wind component, u_g . —: with forest, —: without forest, □: $\alpha = 0.52$, ▢: $\alpha = 0.19$

Turbulent kinetic energy (TKE) normalized with the geostrophic wind component, u_g , is plotted in Fig. 7. Both, the resolved (k_{res}), the SGS (k_{SGS}) and the total ($k_{total} = k_{res} + k_{SGS}$) turbulent kinetic energy are included in the figure. It is shown that the total TKE in the forest case is generally larger. Only within the canopy the without-canopy case shows greater TKE values, which is not surprising, since the presence of the forest strongly hampers the turbulent kinetic energy. For the forest case, the highest levels of k_{total} are reached right above the canopy top, while in the without-canopy case the highest levels are observed closer to the ground. As turbulence is generated by wind shear, it is a rather expected outcome that the highest TKE levels coincide with the regions of the largest velocity gradients (see Fig. 6). Moreover, one can observe that k_{SGS} is generally only a small contribution to k_{total} , except for the without-canopy case at the ground and for the with-canopy case right above the forest.

Turbulence intensities of the streamwise and the vertical velocity components indicate that the turbulence levels are more than doubled by the presence of the forest (not shown here). For the height $y/h = 4.5$, the forest case shows turbulence intensities as large as $I_u = 19.9\%$ and $I_v = 11.6\%$. Without the forest values of merely $I_u = 8.6\%$ and $I_v = 4.8\%$ are reached at the same height. The design criterion proposed by

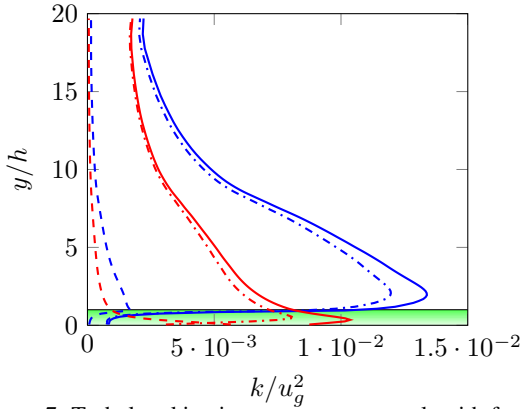


Figure 7: Turbulent kinetic energy. —: total, with forest; - - - : resolved, with forest; - - : modeled, with forest; —: total, without forest; - - - : resolved, without forest; - - - : modeled, without forest

the IEC is $I_u = 16\%$ for the strongest class of wind turbines nowadays (IEC, 2005).

The vertical shear stress is compared for both cases in Fig. 8. The stress in the forest case proves to be significantly larger throughout the entire domain. At the canopy top, the stress in the forest case is more than double as large as for the case without forest at the same height. This result is in line with the findings for turbulence intensities and it implies that the forest flow is much more efficient at momentum transport than the case with lower roughness. Patton et al. (2003) found an increase of merely 22% in a LES comparison of with- and without canopy flows under unstable stratification. They, however, used a coarser vertical grid resolution than we used here, which may explain the differences to a certain degree. Furthermore, they used a different atmospheric stability, which might add to the discrepancy.

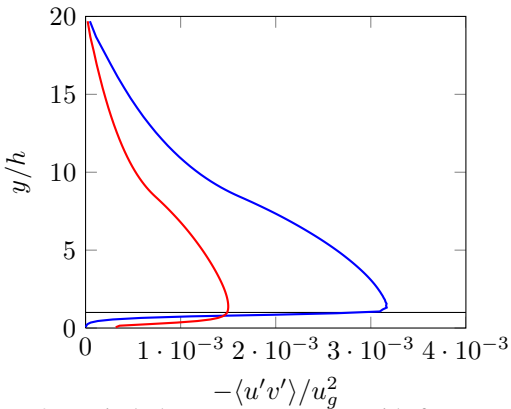


Figure 8: Vertical shear stress. —: with forest, —: without forest

With the help of quadrant analysis, the four contributions to shear stress can be identified. In this technique, up- and downward momentum transfer motions are called ejections and sweeps, respectively. Ejections are events from the second quadrant ($u' < 0, v' > 0$) that carry low-momentum air upwards. Sweeps are events that relate to the fourth quadrant ($u' > 0, v' < 0$) that transport high-momentum air

downwards. The contributions from quadrants 1 and 3 are called the inward and outward interactions. Many research groups have employed this technique to investigate the turbulence structure of numerical or field experiments (Shaw et al., 1983; Su et al., 1998; Finnigan et al., 2009). The interested reader is referred to those references for detailed information on the technique. Here, the technique is used to highlight the importance of sweeps and ejections in momentum transport.

Figure 9 shows the ratio of the contributions by sweeps and ejections to the total shear stress $-\langle u'v' \rangle$. For the with-canopy case, a clear peak can be seen in the upper layers of the canopy ($y/h = 0.8$). This indicates that sweeps dominate over ejections in that region. Physically, this means that the upper region of the forest is mainly penetrated by high-momentum air coming from aloft. A possible explanation of the findings may be that inside the forest the vertical velocity fluctuations are strongly damped, making ejections unlikely. Also above the forest, sweeps play the more important role in momentum transport. Above a height of $y/h = 4.5$, ejections become more and more important. This is in line with findings of other research groups (Shaw et al., 1983; Su et al., 1998; Yue et al., 2007; Finnigan et al., 2009). Deep inside the forest, both ejections and sweeps contribute equally much to the total shear stress. In the case without the forest, sweeps and ejections are roughly equally important for most part of the domain. However, sweeps become the dominant means of momentum transport as the ground is approached. While the latter case shows behavior typical for a rough wall boundary layer as pointed out by Raupach (1981) and Raupach et al. (1991), the behavior in the forest case is a significantly different one.

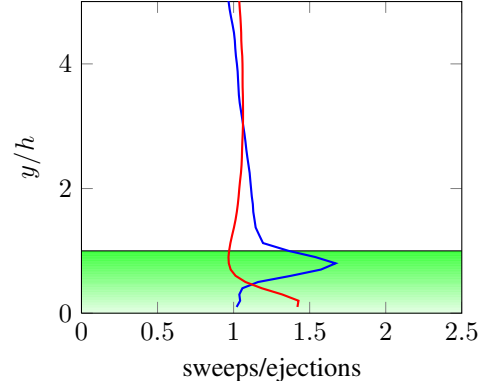


Figure 9: Ratio of the contributions of sweeps to ejections to the total shear stress $-\langle u'v' \rangle$. —: with forest, —: without forest

As already mentioned, sweeps are characterized by events carrying high-momentum air downwards ($u' > 0, v' < 0$). In a sweep dominated case, the probability density function of the time history of the velocity fluctuations will be skewed towards these conditions. Since both cases (with and without forest) are dominated by sweeps near the ground, the skewnesses are expected to be positive and negative for the streamwise

and vertical velocity components, respectively. The skewness plots in Fig. 10 confirm the expectation for the lower region of the domain. For the forest case, it can be seen that the Sk_u goes from positive values at the canopy top to negative values for heights above $y/h \approx 6$. When no forest is present, Sk_u does not show negative values for the entire height of the domain. Wind tunnel measurements by Raupach (1981) indicate that the streamwise skewness should go to negative values higher up in the boundary layer. Possibly, this effect is not captured here, because of the limited domain height of only 400m, which does not permit the simulation of the entire ABL. The vertical skewness shows the reverse behavior: near the ground Sk_v is negative increasing to positive values above $y/h \approx 6$. Measurements by Raupach (1981), Raupach et al. (1991) and large-eddy simulations by Moeng (1984) seem to confirm that behavior. The influence of the canopy is most clearly visible in the plots of streamwise skewness. A sharp peak is shown at canopy height, which must clearly be due to the influence of the forest, as it is not present in the without-canopy case. Similar behavior of the skewness in LES of a forest has been shown by e. g. Dupont and Brunet (2008a). They also found that inside the forest, Sk_u quickly assumes slightly negative values, which can also be observed in Fig. 10. Dupont and Brunet (2008a) report that this phenomenon gets more pronounced with increasing LAI. Without the forest, the streamwise skewness assumes its highest values at the ground.

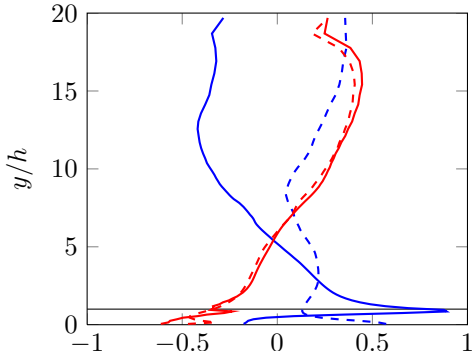


Figure 10: Skewness. —: Sk_u , with forest, - - -: Sk_u , without forest, —: Sk_v , with forest, - - -: Sk_v , without forest

The flatness (or kurtosis) of a signal is a measure of how frequent extreme events occur. Computing the flatness for the velocity fluctuations of the ABL provides then information about whether large or small events dominate the turbulent wind. Thus, it may contain important information about wind turbine loads. For a Gaussian distribution of turbulent fluctuations, the flatness should assume a value of $F \approx 3$. Figure 11 displays the flatness distribution with height for the streamwise and vertical velocity components. As already observed for the skewness in Fig. 10, the flatness

of the vertical fluctuations above the canopy height does not seem to be influenced much by the presence of the forest. Differences become more clear within the canopy only. While the non-forest case shows a steady decrease of flatness up to $y/h = 1$, the case with forest exhibits a kink at $y/h = 0.75$. This kink has not been observed in the simulations by Dupont and Brunet (2008a) and might be related to insufficient statistical averaging. Both cases show strongly non-Gaussian behavior for the region near the ground and for greater heights ($y/h > 10$). The same behavior has been observed by Raupach et al. (1986) in a wind tunnel study on an artificial canopy, even though higher flatness values were measured near the ground ($F_v \approx 7$).

In the streamwise direction, the without-canopy case shows Gaussian values of $F_u \approx 3$ for most of the domain, except very close to the ground. When considering the canopy in the simulation, the flatness of the streamwise velocity assumes values of about 3.5 near the ground and above $y/h \approx 8$. Additionally, a strong peak with values of $F_u = 4.2$ is shown at $y/h = 0.9$. Numerical simulations by Dupont and Brunet (2008a) and Dupont et al. (2011) report the same behavior. Also the wind tunnel study by Raupach et al. (1986) confirms these values. However, higher peak values are usually measured in the field. For example, Baldocchi and Meyers (1988) found peak values of about $F_u \approx 7$ for measurements in a deciduous forest. Dupont and Patton (2012) report peak values of $F_u \approx 8$ for measurements in a fully leaved walnut orchard. The presence of the canopy-top peak in the streamwise flatness of the forest case suggests that infrequent, but extreme events exist in this region. Together with the knowledge gained from the skewness plots, it can be stated that these infrequent, but strong events must be downward-moving gusts (sweeps). In terms of a wind turbine the occurrence of intermittent extreme events may induce potentially harmful loads and should therefore be taken into account in the design process.

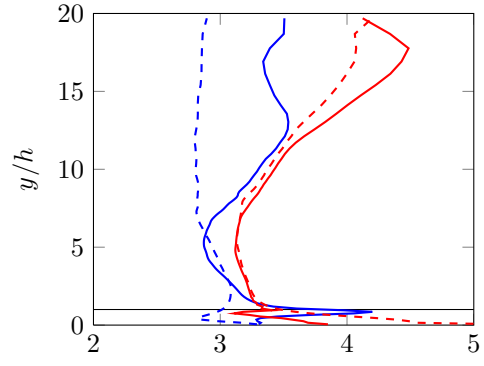


Figure 11: Flatness. —: F_u , with forest, - - -: F_u , without forest, —: F_v , with forest, - - -: F_v , without forest

To further highlight the importance of infrequent

large scale fluctuations in the forest case, the time fractions of the fluctuations exceeding a certain threshold are calculated for the two cases. As the threshold value, the root-mean-square (RMS) of the forest case, i. e. $u'_{rms,F}$ or $(u'v')_{rms,F}$, is used at every height. It can be seen in Fig. 12 that events larger than the RMS value of the streamwise velocity fluctuation are encountered around 32% of the time in the forest case, regardless of the height. At a height of $y/h = 0.8$, a minimum of exceedences is counted. This emphasizes that infrequent, large scale fluctuations are present at that height. For the without-canopy case, the streamwise fluctuations are considerably smaller, exceeding the RMS value of the forest simulation only in 16% of the time up to a height of $y/h \approx 8$ from where on the time fraction increases to about 36% at the top of the domain. Below canopy height, however, the case without forest shows exceedences for about 85% of the time. This is caused by the fact, that the velocity fluctuations are considerably reduced in the with-canopy case due to the presence of the forest. Consequently, also the RMS value of fluctuations is small inside the forest. Hence, Fig. 12 does not imply that the velocity fluctuations in the without-canopy case increase near the ground, but rather that the velocity fluctuations in the canopy case are much smaller there. The same analysis can be made for the shear stress, as plotted in Fig. 13. The forest case shows more frequently large instantaneous shear stress than the case without forest for the entire domain above the forest. It exceeds $(u'v')_{rms,F}$ for about 20% of the time. In the upper layer of the canopy, the time fraction exhibits a minimum. This result again points out the intermittent nature of momentum transport in the upper canopy. In the without-canopy case, the shear stress is mostly smaller than the RMS value of the forest shear stress. The larger time fraction of exceedences near the ground is now not only due to small threshold values, but also due to larger shear stress in the non-forest case in that region (compare the mean values in Fig. 8).

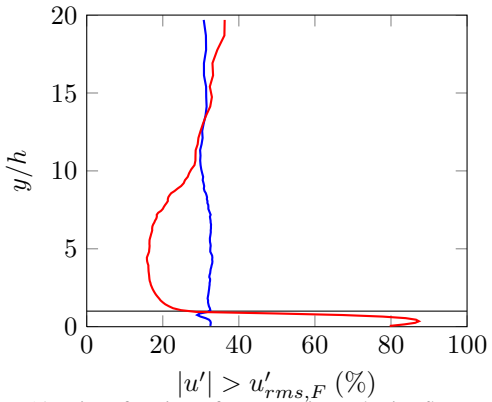


Figure 12: Time fraction of streamwise velocity fluctuations exceeding $u'_{rms,F}$. —: with forest, —: without forest

5 Conclusions

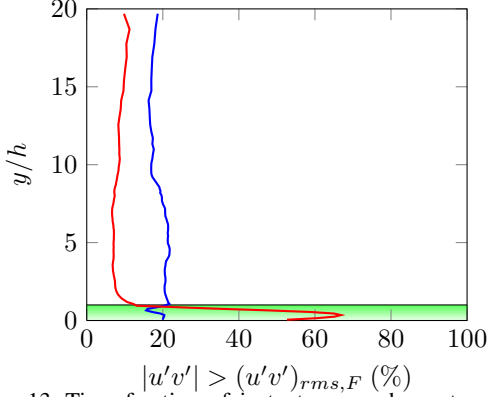


Figure 13: Time fraction of instantaneous shear stress exceeding $(u'v')_{rms,F}$. —: with forest, —: without forest

As an effort to investigate the influence of a forest on the neutral atmospheric boundary layer, two large eddy simulations were performed. One of the simulations explicitly accounted for the forest through a drag force representative of the effect of the trees. In the other simulation, the forest was disregarded and a low-roughness surface was assumed at the ground. The results from the LES with forest were in good agreement with data from field measurements obtained in southern Sweden. Comparing the cases with and without the forest, it was found that the turbulent kinetic energy and the turbulence intensity are considerably increased by the presence of the plants. Values of turbulence intensity at hub-height of an imaginary wind turbine were more than doubled from the without- to the with-canopy case. The IEC design criterion for the strongest class of wind turbines was exceeded in the forest case. Furthermore, it could be shown that the wind shear is considerably increased by the presence of a forest, so that also the second wind turbine design criterion proposed by the IEC is greatly exceeded. With the help of quadrant analysis, the different behavior of the two cases in terms of sweeps and ejections could be pointed out. The without-forest case exhibited typical behavior for a rough wall boundary layer with sweeps being the dominant means of momentum transport when the ground is approached. In the with-forest case, the momentum transport in the top of the canopy and the layers immediately above is mainly governed by sweeps. The analysis of skewness and flatness suggested the occurrence of intermittent, extreme events, which should be taken into consideration when designing a wind turbine for the use in forest regions.

Acknowledgments

This project is financed through the Swedish Wind Power Technology Center (SWPTC). SWPTC is a research center for the design of wind turbines. The purpose of the center is to support Swedish industry with knowledge of design techniques as well as maintenance in the field of wind power. The Center is funded by the Swedish Energy Agency, Chalmers University

of Technology as well as academic and industrial partners.

References

- Baldocchi, D.D. and Meyers, T.P. (1988), Turbulence structure in a deciduous forest, *Boundary-Layer Meteorology*, Vol. 43, no. 4, pp. 345-364.
- Bergström, H. et al. (2013), Wind Power in Forests - Winds and effects on loads, *Elforsk Rapport*, 13:09.
- Breuer, L., Eckhardt, K. and Frede, H.G. (2003), Plant parameter values for models in temperate climates, *Ecological Modelling*, Vol. 169, no. 2, pp. 237-293.
- Deardorff, J.W. (1972), Numerical investigation of neutral and unstable planetary boundary layers, *Journal of the Atmospheric Sciences*, Vol. 29, no. 1, pp. 91-115.
- Deardorff, J.W. (1980), Stratocumulus-capped mixed layers derived from a three-dimensional model, *Boundary-Layer Meteorology*, Vol. 18, no. 4, pp. 495-527.
- Dupont, S. and Brunet, Y. (2008a), Edge flow and canopy structure: a large-eddy simulation study, *Boundary-Layer Meteorology*, Vol. 126, no. 1, pp. 51-71.
- Dupont, S. and Brunet, Y. (2008b), Influence of foliar density profile on canopy flow: a large-eddy simulation study, *Agricultural and Forest Meteorology*, Vol. 148, no. 6, pp. 976-990.
- Dupont, S. and Brunet, Y. (2009), Coherent structures in canopy edge flow: a large-eddy simulation study, *Journal of Fluid Mechanics*, Vol. 630, pp. 93-128.
- Dupont, S., Bonnefond, J.-M., Irvine, M.R., Lamaud, E., Brunet, Y. (2011), Long-distance edge effects in a pine forest with a deep and sparse trunk space: In situ and numerical experiments, *Agricultural and Forest Meteorology*, Vol. 151, no. 3, pp. 328-344.
- Dupont, S. and Patton, E.G. (2012), Influence of stability and seasonal canopy changes on micrometeorology within and above an orchard canopy: The CHATS experiment, *Agricultural and Forest Meteorology*, Vol. 157, pp. 11-29.
- Finnigan, J.J. (2000), Turbulence in plant canopies, *Annual Review of Fluid Mechanics*, Vol. 32, no. 1, pp. 519-571.
- Finnigan, J.J., Shaw, R.H. and Patton, E.G. (2009), Turbulence structure above a vegetation canopy, *Journal of Fluid Mechanics*, Vol. 637, pp. 387-424.
- Hunt, J.C.R., Kaimal, J.C. and Gaynor, J.E. (1988), Eddy structure in the convective boundary layernew measurements and new concepts, *Quarterly Journal of the Royal Meteorological Society*, Vol. 114, no. 482, pp. 827-858.
- IEC. (2005). IEC 61400-1 Wind Turbines Part1: Design Requirements. Geneva: International Electrotechnical Commission.
- Kanda, M., and Hino, M. (1994), Organized structures in developing turbulent flow within and above a plant canopy, using a large eddy simulation, *Boundary-Layer Meteorology*, Vol. 68, no. 3, pp. 237-257.
- Lalic, B. and Mihailovic, D.T. (2004), An empirical relation describing leaf-area density inside the forest for environmental modeling, *Journal of Applied Meteorology*, Vol. 43, no. 4, pp. 641-645.
- Moeng, C.H. (1984), A large-eddy-simulation model for the study of planetary boundary-layer turbulence, *Journal of the Atmospheric Sciences*, Vol. 41, no. 13, pp. 2052-2062.
- Patton, E.G., Sullivan, P.P. and Davis, K.J. (2003), The influence of a forest canopy on topdown and bottomup diffusion in the planetary boundary layer, *Quarterly Journal of the Royal Meteorological Society*, Vol. 129, no. 590, pp. 1415-1434.
- Raupach, M.R. (1981), Conditional statistics of Reynolds stress in rough-wall and smooth-wall turbulent boundary layers, *Journal of Fluid Mechanics*, Vol. 108, pp. 363-382.
- Raupach, M.R., Antonia, R.A. and Rajagopalan, S. (1991), Rough-wall turbulent boundary layers, *Applied Mechanics Reviews*, Vol. 44, no. 1, pp. 1-25.
- Raupach, M.R., Coppin, P.A. and Legg, B.J. (1986), Experiments on scalar dispersion within a model plant canopy part I: The turbulence structure, *Boundary-Layer Meteorology*, Vol. 35, no. 1-2, pp. 21-52.
- Raupach, M.R., Finnigan, J.J. and Brunet, Y. (1996), Coherent eddies and turbulence in vegetation canopies: the mixing-layer analogy, *Boundary-Layer Meteorology*, Vol. 78, no. 3-4, pp. 351-382.
- Shaw, R.H., Den Hartog G. and Neumann, H.H. (1988), Influence of foliar density and thermal stability on profiles of Reynolds stress and turbulence intensity in a deciduous forest, *Boundary-Layer Meteorology*, Vol. 45, no. 4, pp. 391-409.
- Shaw, R.H. and Patton, E.G. (2003), Canopy element influences on resolved-and subgrid-scale energy within a large-eddy simulation, *Agricultural and Forest Meteorology*, Vol. 115, no. 1, pp. 5-17.
- Shaw, R.H. and Schumann, U. (1992), Large-eddy simulation of turbulent flow above and within a forest, *Boundary-Layer Meteorology*, Vol. 61, no. 1-2, pp. 47-64.
- Shaw, R.H., Tavangar, J. and Ward, D.P. (1983), Structure of the Reynolds stress in a canopy layer, *Journal of Climate and Applied Meteorology*, Vol. 22, no. 11, pp. 1922-1931.
- Sommeria, G. (1976), Three-dimensional simulation of turbulent processes in an undisturbed trade wind boundary layer, *Journal of the Atmospheric Sciences*, Vol. 33, no. 2, pp. 216-241.
- Su, H.B., Shaw, R.H., Paw, K.T., Moeng, C.H. and Sullivan, P.P. (1998), Turbulent statistics of neutrally stratified flow within and above a sparse forest from large-eddy simulation and field observations, *Boundary-Layer Meteorology*, Vol. 88, no. 3, pp. 363-397.
- Watanabe, T. (2004), Large-eddy simulation of coherent turbulence structures associated with scalar ramps over plant canopies, *Boundary-Layer Meteorology*, Vol. 112, no. 2, pp. 307-341.
- Wieringa, J. (1992), Updating the Davenport roughness classification, *Journal of Wind Engineering and Industrial Aerodynamics*, Vol. 41, no. 1, pp. 357-368.
- Yue, W., Meneveau, C., Parlange, M.B., Zhu, W., Van Hout, R. and Katz, J. (2007), A comparative quadrant analysis of turbulence in a plant canopy, *Water Resources Research*, Vol. 43, no.5.